In Vitro Patients' Derived Glioma Culture Model: Identification of Aggressive, Drug Resistant Phenotype Among Low-Grade Gliomas

Syed Sultan Beevi[1]*, Vinod Kumar Verma[1]*, Manas Panigrahi[2], Aishwarya Bhale[1,5], Sailaja Madigubba[3], Radhika Chowdary[4], Radhika Korabathina[1], Sukrutha Gopal Reddy[4]

[1]Cancer Biology Division, KIMS Foundation and Research Centre, KIMS Hospital, Minister Road, Secunderabd, Telangana, India

[2]Department of Neurosurgery, Krishna Institute of Medical Sciences, Minister Road, Secunderabad, Telangana, India

[3]Department of Pathology, Krishna Institute of Medical Sciences, Minister Road, Secunderabad, Telangana, India

[4]Diagnostics Division, Krishna Institute of Medical Sciences, Minister Road, Secunderabad, Telangana, India

[5]Department of Genetics, Osmania University, Hyderabad, Telangana, India

*Corresponding Authors
Syed Sultan Beevi PhD
KIMS Foundation and Research Centre
KIMS Hospitals
1-8-31/1, Minister Road
Secunderbad 500 003
Telangana, India
Tel: 91 40 44885056
Fax: 91 40 27840980
Email: drsyedsultan.b@kfrc.co.in
Vinod Kumar Verma PhD
KIMS Foundation and Research Centre
KIMS Hospitals
1-8-31/1, Minister Road
Secunderbad 500 003
Telangana, India
Tel: 91 40 44885056
Fax: 91 40 27840980
Email: drvinod.v@kfrc.co.in

Abstract

Background: Low-grade gliomas are mostly played down as less fatal malignancy despite the fact that most of them eventually progress to high grade thereby leading to death. *In vitro* glioma cultures have been emerged as a standard model to get insight into phenotypic transformation, drug response and tumor relapse. In this study, attempt was made to establish comprehensive patient-specific short-term cultures comprising of both low-grade and high-grade malignant glioma.

Methods: 50 patients with MRI diagnosed malignant glioma were recruited for this study. Fresh surgical tumor tissues were used for the establishment of primary culture. Patients' samples were analyzed for the presence of IDH1/2 mutations, 1p/19q co-deletion, MIB1 and p53. Established primary glioma culture were evaluated for proliferation rate, sensitivity to temozolomide and expression pattern of Glial-Mesenchymal Transition (GMT) markers.

Results: Short-term glioma cultures were successfully established in 40 clinical samples. Glioma cultures, irrespective of tumor grades, displayed two distinct pattern of growth kinetics – one with shorter doubling time (high-proliferating) and another group with longer doubling time (low-proliferating). Significant distinctive features were noticed between these two groups in terms of response to temozolomide, expression pattern of GMT markers and their association with clinical/pathological features of malignant glioma.

Conclusion: Our findings effectively demonstrated the practicality of development of short-term glioma culture model toward a functional approach for personalized medicine. Our model further revealed the presence of highly proliferative, drug-resistant phenotype among low-grade gliomas. Hence, short-term culture model could be an important prognostic tool to predict patient clinical responses and also provide cue about imminent tumour relapse.

Introduction

Malignant gliomas are the most common intra-axial primary tumors originating from the supporting glial cells of the central nervous system. Gliomas have the third highest cancer-related mortality and morbidity rates among individuals worldwide (1) with an annual incidence of 1 million cases in India (2). The World Health Organization (WHO) classification system categorizes gliomas as grade 1 (biologically benign), grade II (diffuse astrocytoma/oligodendroglioma), grade III (anaplastic astrocytoma) and grade 4 (glioblastoma), based upon histopathologic characteristics such as cytological atypia, anaplasia, mitotic activity, microvascular proliferation, and necrosis (3).

Glioblastoma Multiforme (GBM) is the most studied brain tumor owing to tumor recurrence, treatment resistant and abysmal survival rate. Conversely, low grade gliomas are also equally fatal, even though they have better survival than patients with GBM (4). Most of the low-grade gliomas eventually progress to high grade glioma thereby leading to death in due course. National Cancer Institute data imply that overall survival rate of low-grade glioma patients has not increased significantly despite advancement in treatment strategies. Latest research further reveals that recently discovered tumor markers such as IDH1/2 mutation and 1p/19q co-deletion status have failed to provide information on eventual progression of low-grade to high-grade glioma (5), emphasizing the necessity for new and different prognostic/predictive indicators.

Infiltrative phenotype has long been considered as a contributory factor for clinical aggravation of malignant glioma that manifest as tumour recurrence and therapeutic intractability (6). Such infiltrative features have been explicitly linked to the phenomenon of epithelial-mesenchymal transition (EMT). The role of EMT in non-epithelial tumours like malignant glioma is nonetheless uncertain. However, recent classification of mesenchymal subgroup of GBM strengthen the notion of glial-mesenchymal transition (GMT) similar to EMT-like process in glioma and may contribute to tumour progression, chemo-resistance and tumour relapse regardless of tumour grades (7). Several studies have investigated the expression of EMT markers such as vimentin, TWIST, SNAIL, E-cadherin and N-cadherin in malignant gliomas and demonstrated their apparent role in invasion, drug resistance and tumour recurrence (8-11).

Patient-derived glioma cultures are gradually gaining impetus in brain tumor research and exemplify a way to get insight into prognostic and therapeutic attributes. Such *in vitro* models intently simulate the biological traits of the patient tumor, thus providing an opportunity to apprehend drug resistance, tumor recurrence and response to therapy in a patient-distinctive manner. Such individual models enable the most precise response and resistance extrapolation outside the patient (12).

Most of the *in vitro* glioma models referred in the literature are of high-grade gliomas (13, 14). Paradoxically, studies on low-grade glioma culture are very much limited. Given that, most of the low-grade gliomas eventually progress to high grade glioma over a period of time, we hypothesize that groups of cells within low-grade tumor could have propensity to set off tumor relapse despite treatment and such gliomas would have high proliferative ability with apparent resistance to chemotherapeutic drugs and would present distinct GMT expression profile.

To test our hypothesize, we established the primary culture of both low-grade and high-grade gliomas and evaluated their proliferative status in terms of population doubling analysis, sensitivity to temozolomide and expression pattern of GMT markers. We further assessed the association of proliferation rate of gliomas with IDH1/2 mutation, 1p/19q co-deletion, p53 and MIB1 expression.

Materials and methods

All the fine biochemicals were procured from Sigma-Aldrich, USA, unless otherwise stated. Cell culture media and supplements including Fetal Bovine Serum (BSA), glutamine and pencillin-streptomycin solution were purchased from Gibco, Thermo Fischer Scientific, USA and antibodies (primary and secondary) were procured from Invitrogen, Thermo Fischer Scientific, USA. Cell culture plates and flasks were from Effendorf, Germany.

Patients selection

50 patients with MRI diagnosed probable malignant glioma, who visited the Department of Neurosurgery, Krishna Institute of Medical Sciences, Telangana, India, between December 2018 and January 2020 were recruited before their scheduled surgery. This study was approved by the Institutional Research Advisory Board and Ethics Committee. Prior informed consent was obtained in

written form from all patients. The study was conducted in accordance with general acceptance guidelines for the use of human material.

Intraoperative tissue collection

Resection specimen of glioma tumor was divided in two parts, with one part in a sterile collection medium for the establishment of primary culture and other part placed in buffered formalin for histological and pathological analysis.

Establishment of primary glioma culture

Tumor tissues received in sterile carrier medium was processed immediately within 2h upon arrival in the laboratory. Briefly, tumor tissue was minced by scalpel in PBS and digested with 0.1% collagenase I for 30 minutes at 37°C with intermittent shaking. Collagenase I activity was arrested by the addition of FBS and passed through a cell strainer (100 μm) to obtain a single cell suspension. Cells were washed with PBS and seeded in T25 culture flask containing DMEM/F12 cell culture media supplemented with 10% FBS, 10ng/mL EGF/FGF-2, 2mM L-glutamine and 1% penicillin-streptomycin and allowed to adhere to their surface for 72 h at 37°C in 5% CO2. Unattached cells were removed through media change after 72 h and allowed the adherent cells to reach confluence of about 80% before trypsin treatment and passaging. Cells were passaged 4-6 times and expanded for subsequent analysis.

Morphological characterization of primary glioma cells

Glioma cells were cultured in T25 flasks to a confluence of 60 – 80% and morphology was assessed under an inverted phase contrast microscope. Cells were photographed and processed using the cellSens software (Olympus, Japan).

Population Doubling Analysis

Cells were seeded at the density of 2 x 10^3 cells per cm2 of surface area and incubated overnight at 37°C in 5% CO2. Plates were counted in duplicates every 24 h for seven consecutive days. Results were plotted on a linear scale as cell number versus time. Population doubling time (PDT) was calculated from the linear part of the curve using this equation: (t2 – t1)/3.32 x (log n2 – log n1), where t is time and n is number of cells.

Sensitivity to Temozolomide

Cells (5 x 10^3) were plated in 100µl DMEM/F12 media per well in triplicate in 96 well flat bottom culture plates and allowed to adhere for 18h. Cells were then exposed to Temozolomide (in the concentration range of 2.5mM - 156µM) for 48h. Equal volume of DMSO were added to cells serving as control. After 48h, cells were treated with 20µl of MTT (3-(4,5-dimethylthiazolyl-2)-2,5-diphenyltetrazolium bromide) at a concentration of 5mg/mL in PBS and incubated for 4h. MTT containing media were discarded, added with 100µl of DMSO, vibrated for 10 min to dissolve the formazan crystals and the absorbance was measured at 570nm by an ELISA microplate reader. The degree of inhibition of cell proliferation in each sample was calculated by the following formula: Inhibition of cell proliferation (%) = (1 – absorbance of the experimental group/absorbance of the control group) x 100. Half maximal inhibitory concentration (IC50) was calculated by using regression analysis from GraphPad Prism.

Expression pattern of GMT markers by Immunofluorescence

Glioma cells were cultured on 22x22mm square coverslips into 6-well culture plates and allowed to adhere overnight at 37°C in 5% CO2. Cells were washed in PBS, fixed for 20 min at room temperature in 4% paraformaldehyde in PBS. After fixation, cells were permeabilized with 0.1% Trition X-100 for 10 min and blocked with 5% bovine serum albumin for 1h at room temperature. Primary antibodies GFAP (rat anti-human IgM at 1:200 dilution), Vimentin (mouse anti-human IgM at 1:100), TWIST (mouse anti-human IgM at 1:100), E-cadherin (mouse anti-human IgM at 1:100), N-cadherin (mouse anti-human IgM at 1:100) and cMyc (mouse anti-human IgM at 1:100) were added and incubated overnight at 4°C. Cells were rinsed 3x with PBS and incubated with fluorescence-labeled (Alexa488/Alexa 594) secondary antibody and incubated at room temperature, protected from light for 1h. Cells were rinsed 3x with PBS and mounted with VECTASHIELD mounting medium containing DAPI. The slides were analyzed by fluorescence microscopy (Olympus, Japan) and image processing was carried out using cellSens software. Cells were observed at different microscopic magnifications to make the precise assessment of percentages of stained cells. The entire slides were evaluated to avoid a biased selection of more or less intense staining areas. Quantitative scoring was done based on the percentage of positive cells and defined as: 0 for <10% positive cells (negative), 1 for 10 – 25% (low

expression), 2 for 25 – 50% (moderate expression), 3 for 50 – 75% (strong expression) and 4 for >75% (intense expression)

Pathological examination and immunohistochemistry of the patient glioma tissue

The tumor tissue was fixed in 10% buffered formalin, dehydrated with ethanol gradient, permeabilized with xylene and paraffin embedded. Then, serial 5μm thick sections were cut, deparaffinized with xylene, hydrated with ethanol gradient and stained with hematoxylin and eosin (H & E). Meanwhile, immunohistochemical staining was performed for IDHR132, p53 and MIB-1 detection. Endogenous peroxidase inactivation was carried out with 3% H2O2, and antigen retrieval was performed in a microwave. Afterward, primary antibodies were added to each slide at appropriate dilutions, and the sections incubated with biotin-labeled secondary antibodies for 10 min. The final signals were developed using the 3,3'-diaminobenzidine substrate (DAB). The sections were analyzed by optical microscopy after counterstaining with hematoxylin.

IDH mutational analysis

Genomic DNA was isolated from FFPE tissue sections using QIAamp DNA FFPE tissue kit according to manufacturer's instructions. Concentration of isolated DNA was determined with the NanoDrop100. All the samples were analyzed for the mutation using Qiagen IDH1/2 RGQ PCR kit, in the following loci: IDH1R132 (exon4), IDH1R100 (exon4) and IDH2R172 (exon 4). The desired genomic regions were amplified by qPCR using specific primers and probes, according to manufacturer's instruction.

1p/19q co-deletion

Co-deletion of 1p and 19q in tumor tissue samples were evaluated with fluorescence in situ hybridization (FISH) with locus-specific probes, LSI 1p36/1q25 or LSI 19q13/19p13. A positive result for 1p/19q co-deletion was assessed as the loss of 1p36 or 19q13 signal in more than 50% of nuclei.

Statistical analysis

Clinical and biochemical data were expressed as mean ± standard deviation. Chi-square test for independence ($\chi 2$) and Pearson correlation coefficient (r) were applied to determine the association between proliferation status and clinical/pathological features of gliomas. The p value <0.05 was considered as statistically significant.

Results

Clinical and pathological characteristics of glioma patients

50 patients with MRI-diagnosed primary malignant glioma were enrolled for our study before their curative resection. Out of 50 patients, five were excluded from the study as their later histological analysis revealed the presence of brain tumors other than malignant glioma. Of the 45 patients, 14 were in grade II, 9 and 22 were in Grade III and IV respectively. Detailed clinical and pathological characteristics of the glioma patients inclusive of IDH mutation and 1p/19q co-deletion status is presented as Table 1.

Establishment of primary glioma culture

All the samples were processed immediately within 2h upon arrival at laboratory. Samples were digested enzymatically and single cell suspension were grown as monolayer culture in EFF/FGF-2 enriched media. Establishment of monolayer culture was successful in 89% (40/45) of the samples. Five samples (two each in grade II & grade III and one sample in grade IV) either failed to attach or cease to grow after first passage. Morphological evaluation, PDT, temozolomide sensitivity testing and GMT markers analysis were performed mostly between passage 4 – 6 to minimize genomic instability due to long-term culture process.

Morphological Evaluation

All the established primary glioma cells were micro-photographed to assess their morphology. Representative images of the cultured glioma cells are depicted as Figure 1. Under phase contrast microscope, primary culture showed cells with variable morphological features, predominantly having dendritic-like and fibroblastic-like phenotype. There was no apparent difference in morphology between low-grade and high-grade glioma culture.

Population Growth Analysis

Estimation of PDT by application of the exponential growth equation (15) was employed to quantitate the proliferative capacity and intrinsic growth properties of the cultured primary glioma cells. Based on the PDT, cultured cells were categorized to group with high proliferation rate (having PDT < 72h) and to group with low proliferation rate (having PDT > 72h). Glioma culture exhibited diverse proliferative

capacity and intriguingly, high and low proliferating gliomas were observed irrespective of tumor grades. By and large, 19 samples were found to be of high proliferating and 21 samples of low proliferating group. When high and low-proliferating cultures were categorized grade-wise, grade IV samples presented with a greater number of low-proliferating cultures and whereas grade II samples had more number of high-proliferating cultures (presented as Figure 2A) with almost equivalent distribution of high and low-proliferating group in grade III samples. Interestingly, it was observed that doubling time was significantly shorter in high-grade as compared to low-grade of high-proliferating cultures and vice versa in low-proliferating group (Figure 2B).

Sensitivity of primary glioma cells to Temozolomide

The sensitivity of each established primary glioma cells was assessed towards temozolomide with its indicated concentration (as mentioned in materials and methods). Inhibitory Concentration (IC50) value was calculated for all the tested sample and categorized grade-wise with respective to their proliferative capacity (summarized in Table 2). Samples belonging to low proliferating group were showing significantly lower IC50 as compared to high proliferating cultures. Essentially, IC50 of low proliferating grade II and grade IV cultures were within the tested concentration of 0.156 – 2.5 mM, when compared with high proliferating cultures where it was found to be in the range of 3 – 9 mM. Notwithstanding, all grade III cultures were highly resistant to TMZ with IC50 ranging between 4.5 – 13.3 mM, irrespective of their proliferation rate.

Glial-Mesenchymal Transition (GMT) markers expression

Expression pattern of GMT markers such as GFAP, vimentin, TWIST, E-cadherin, N-cadherin and cMyc were evaluated in three samples each from both high and low proliferating category comprising of grade II to grade IV and presented as Figure 3. There was a significant difference in the expression pattern of GMT markers between high and low proliferating cultures. Broadly, low proliferating cultures showed null to low expression of GFAP, low expression of vimentin, TWIST, N-cadherin and cMyc and null expression of E-cadherin. Whereas in high proliferating cultures, there was strong expression of all markers including E-cadherin. However, grade IV high proliferating cultures showed exceptionally strong distinctive E-cadherin staining as compared to grade II and III. Besides, moderate

to strong nuclear cMyc expression was observed in all high proliferating cultures as opposed to low cytoplasmic expression in low proliferating cultures.

IDH1/2 mutation and 1p/19q co-deletion status

IDH1/2 mutations and 1p/19q co-deletion status were detected in tissue specimens from each patient and determined their frequency with respect to high and low proliferating culture groups (Table 2). IDH1R132 mutations were detected in all samples from patients with grade II regardless of its high or low proliferation status of glioma culture. Most of the samples tested positive for IDH1R132H mutation except two samples which showed positivity for IDH1R132C. Conversely all grade IV samples were tested negative for IDH1/2 mutation and only one sample from high proliferating group of grade III showed positivity for IDH1R100. Complete 1p/19q co-deletion was detected in 6 out of 12 grade II samples. However, there was only one sample out of 7 in grade III showed co-deletion and none in case of grade IV samples.

MIB1 and p53 expression in FFPE tissue section

MIB1 expression was found to be negative in all the grade II sample irrespective of proliferation status of the primary glioma culture. However, all grade III and IV samples showed differential degree of expression that were categorized as weak (1+), moderate (2+) and strong (3+), illustrated in Table 1. In case of p53, proliferation status of culture appeared to play a considerable role as the number of positivity was more for those patients who had high proliferating glioma cells in cultures (14 positive out of 19 samples) and less for those with low proliferating cultures (6 positive out of 21 samples).

Association of clinical and pathology features with proliferation status of primary culture

Two-sided $\chi 2$ test to evaluate the association of proliferative ability of primary culture with age, sex, IDH mutation, 1p/19q co-deletion, p53 and MIB1 expression revealed that proliferation ability of primary culture was significantly associated with 1p/19q co-deletion ($p = 0.0497$) and p53 expression ($p = 0.0044$), but not with age, gender, IDH1/2 mutation and MIB1 expression (Table 4). Besides, simple linear regression analysis (Figure 4) revealed that significant correlation was found in case of 1p/19q co-deletion ($p = 0.05$) and p53 expression ($p = 0.05$), thereby substantiating the impact of proliferation rate of cultured primary glioma cells on their pathological features.

Discussion

Therapeutic strategy and ensuing prognosis of malignant gliomas differ considerably depending on the tumour grade and molecular biomarkers (16). Despite newer treatment modalities, the impact on the local control of tumour is marginal and survival statistics is not quite remarkable. The reason for treatment failure could be the presence of quiescent cells that could later transform into more aggressive phenotype, setting off tumour relapse (17). Unfortunately, trigger for these transformation is poorly understood and there is no therapeutic approach to delay or stop this process. Of late, *in vitro* patient-specific glioma cultures have emerged as a standard model to get insight into these crucial aspects.

Although, a large volume of studies pertaining to *in vitro* GBM model has been published (13, 14, 18,19) low-grade glioma models remains relatively unexplored. In this study, we successfully established *in vitro* primary culture of both low-grade and high-grade gliomas from fresh surgical tumour materials and evaluated their growth kinetics along with TMZ sensitivity and GMT expression pattern. Morphologically, there was no distinctive features noticed between low-grade and high-grade as both cultures showed mixed cell population, mostly of dendritic and fibroblastic phenotypes. Intriguingly, there was a conspicuous differences in the proliferation rate of glioma cultures, some being doubled swiftly in less than 72 h and others proliferating at a much lesser pace. We noticed this unique growth trend irrespective of tumour grades and subsequently categorized as high-proliferating and low-proliferating cultures. Moiseeva et al (19) have reported the trend similar to our findings, albeit in the proliferation rate of high-grade GBM. In contrast, Mullins et al (13) have reported no precise differences in the growth kinetics of GBM cell lines established from fresh and frozen surgical materials.

It is well known that every tumour follows a well-defined logistic growth curve and differs in line with quiescent tumour cells (20). There was clear evidence of shortened doubling time, regardless of tumour grades, in certain proportion of our studied patients. We presume that quiescent tumour cells not engaged in a cell cycle owing to lack of oxygen or nutrients triggered into proliferation under *in vitro* culture conditions and this could plausibly indicate the impending progression of histological characteristics to a more aggressive phenotype.

Temozolomide (TMZ) is part of the standard of care for adjuvant therapy of malignant gliomas, despite the fact that at least 50% of the TMZ-treated patients eventually develop resistance to TMZ (21). Under

such milieu, we intended to ascertain whether culture's proliferative status could have impact on the TMZ sensitivity. Thenceforth, we evaluated the half maximal inhibitory (IC50) concentration of TMZ on all established glioma cultures. Low proliferating cultures of grade II and IV tend to be more sensitive to TMZ with IC50 values lying within the tested concentration when compared with high proliferating cultures. However, all the grade III samples showed intense resistance to TMZ irrespective of their proliferation status. We presumed that high-proliferating cultures could have had drug tolerant cells, that being in a specific cellular state allowing them to endure drug treatment and eventually giving rise to highly aggressive phenotype.

Mesenchymal differentiation or transformation contribute to a cellular ability to evade the effects of chemotherapies and promote drug resistance in several cancers (22, 23). Although the contribution of EMT in non-epithelial tumours like glioma is still debatable, we assume that GMT as a complement of EMT could be an essential process in glioma progression and promote drug resistance. Several studies have reported the modulation of distinctive EMT markers during the development of drug resistance in GBM (9, 24). We observed a notable variation in the expression profile of GMT markers amongst low-proliferating and high-proliferating cultures. Distinctive features among them were concurrent strong expression of GFAP and N-cadherin in high-proliferating cultures regardless of tumour grades. Besides, we noticed strong expression of E-cadherin in grade IV high-proliferating cultures. While it has been suggested that downregulation of E-cadherin and upregulation of N-cadherin is the hallmark of EMT (25), loss of E-cadherin may not be a necessary phenomenon for EMT as restoration of E-cadherin expression in E-cadherin negative malignant cells did not reverse the EMT process (26). Our study thus substantiate the potential link between proliferation rate of tumour cells and expression profile of GMT markers that collectively could be responsible for the drug resistance observed in the high-proliferating glioma cultures.

Another striking observation in our study was the nuclear expression of c-Myc in high-proliferating cultures as opposed to cytoplasmic expression in low-proliferating cultures. Although high expression of c-Myc was previously described in a large proportion of glioblastomas (27), information on cellular localization was sparse. Gurel et al (28) have reported that increased nuclear expression of c-Myc could be a significant oncogenic event driving initiation and progression in human prostate cancer. Given that

fact, we presume that nuclear c-Myc expression could very well be served as a predictive marker for tumour recurrence and/or drug resistance.

Subsequently we sought to assess the frequency of IDH1/2 mutation, 1p/19q co-deletion status and other pathological features with respect to proliferation rate of cultured gliomas. In accordance with several previous reports (29, 30), IDH1/2 mutations were essentially found among grade II with negligible association to proliferation rate. Similarly MIB1 expression were found exclusively in the high-grade, but not in low-grade, irrespective of proliferation status of glioma cultures. However, we found significant association of 1p/19q co-deletion and p53 expression with proliferation rate, thereby suggesting their plausible link to the intrinsic growth properties of malignant gliomas. .

Conclusion

Low-grade gliomas are rather slow-growing infiltrative primary brain tumours that perpetually undergo malignant transformation. Risk stratification and prognostication in low-grade gliomas are less distinct when compared with GBM. In this study, we effectively demonstrated the practicality of development of short-term glioma culture model toward a functional approach for personalized medicine. Our model revealed the presence of highly proliferative, drug-resistant phenotypes among low-grade gliomas. Similarly, less aggressive drug-sensitive phenotypes were found among high-grade gliomas. However, cultures established from grade III behaved in an unique manner in terms of response to temozolomide regardless of their proliferation status. Clinical significance of gliomas with differential growth kinetics and drug response is to be ascertained with effective patients' follow-up and survival analysis, that is underway in our laboratory. Nevertheless, our short-term glioma model could be a constructive tool for the management of low-grade gliomas and could also provide cue about imminent tumour relapse.

References

1. Ostrom QT, Bauchet L, Davis FG, Deltour I, Fisher JL, Langer CE, et al. The epidemiology of glioma in adults: a "state of the science" review. Neuro Oncol. 2014; 16: 896-913.
2. Yeole BB. Trends in the brain cancer incidence in India. Asian Pac J Cancer Prev. 2008; 9: 267-270.

3. Louis DN, Perry A, Reifenberger G, Deimling A, Figarella-Branger D, Cavenee WK, et al. The 2016 World Health Organization Classification of Tumours of the Central Nervous System: a summary. Acta Neuropathol. 2016; 131:803.
4. Claus EB, Horlacher A, Hsu L, Schwartz RB, Dello-Iacono D, Talos F, et al. Survival rates in patients with low-grade glioma after intraoperative magnetic resonance image guidance. Cancer. 2005; 103: 1227-1233.
5. Claus EB, Walsh KM, Wiencke JK, Molinaro AM, Wiemels JL, Schildkraut JM, et al. Survival and low-grade glioma: the emergence of genetic information. Neurosurg Focus. 2015; 38: E6.
6. Diksin M, Smith SJ, Rahman R. The Molecular and Phenotypic Basis of the Glioma Invasive Perivascular Niche. Int J Mol Sci. 2017; 18: 2342.
7. Behnan J, Ginocchiaro G, Hanna G. The landscape of the mesenchymal signature in brain tumors. Brain. 2019;142:847-866.
8. Nowicki MO, Hayes JL, Chiocca EA, Lawler SE. Proteomic Analysis Implicates Vimentin in Glioblastoma Cell Migration. Cancers. 2019; 11: 466.
9. Liang H, Chen G, Li J, Yang F. Snail expression contributes to temozolomide resistance in glioblastoma. Am J Transl Res. 2019; 11: 4277-4289.
10. Elias MC, Tozer KR, Silber JR, Mikheeva S, Deng M, Morrison RS et al. TWIST is expressed in human gliomas and promotes invasion. Neoplasia. 2005; 7: 824-837.
11. Noh MG, Oh SJ, Ahn EJ, Kim YJ, Jung TY, Jung S et al. Prognostic significance of E-cadherin and N-cadherin expression in Gliomas. BMC Cancer. 2017; 17: 583.
12. da Hora CC, Schweiger MW, Wurdinger T, Tannous BA. Patient-Derived Glioma Models: From Patients to Dish to Animals. Cells. 2019 ;8: 1177.
13. Mullin CS, Schneider B, Stockhammer F, Krohn M, Classen CF et al. Establishment and characterization of primary glioblastoma cell lines from fresh and frozen material: A detailed comparison. PLoS ONE. 2013; 8: e71070.
14. Ledur PF, Onzi GR, Zong H, Lenz G. Culture conditions defining glioblastoma cells behavior: what is the impact for novel discoveries? Oncotarget. 2017;8: 69185-69197.

15. Greenwood SK, Hill RB, Sun JT, Armstrong MJ, Johnson TE, Gara JP, et al. Population doubling: A simple and more accurate estimation of cell growth suppression in the in vitro assay for chromosomal aberrations that reduces irrelevant positive results. Environ Mol Mutagen. 2004; 43:36-44.
16. Olar A, Aldape KD. Biomarkers classification and therapeutic decision-making for malignant gliomas. Curr Treat Options Oncol. 2012; 13:417-436.
17. Whittle IR. The dilemma of low grade glioma. J Neurol Neurosurg Psychiatry. 2004;75 (Suppl II): ii31–ii36.
18. Mullins CS, Schneider B, Lehmann A, Stockhammer F, Mann S, Classen CF, et al. A Comprehensive Approach to Patient-individual Glioblastoma Multiforme Model Establishment. J Cancer Sci Ther. 2014; 6: 177-187.
19. Moiseeva NI, Susova OY, Mitrofanov AA, Panteleev DY, Pavlova GV, Pustogarov NA, et al. Biochemistry (Moscow) 2016; 81: 628-635.
20. Maurice Tubiana. Tumor Cell Proliferation Kinetics and Tumor Growth Rate, Acta Oncologica 1989; 28:113-121.
21. Lee SY. Temozolomide resistance in glioblastoma multiforme. Genes Dis. 2016;3:198-210.
22. Prieto-Vila M, Takahashi RU, Usuba W, Kohama I, Ochiya T. Drug Resistance Driven by Cancer Stem Cells and Their Niche. Int J Mol Sci. 2017;18: 2574.
23. Scheel C, Eaton EN, Li SH, Chaffer CL, Reinhardt F, Kah KJ, et al. Paracrine and autocrine signals induce and maintain mesenchymal and stem cell states in the breast. Cell. 2011;145:926-940.
24. Chen C, Han G, Li Y, Yue Z, Wang L, Liu J. FOX01 associated with sensitivity to chemotherapy drugs and glial-mesenchymal transition in glioma. J Cellular Biochem. 2019; 120: 882-893.
25. Loh CY, Chai JY, Tang TF, Wong WF, Sethi G, Shanmugam MK, Chong PP, Looi CY. The E-Cadherin and N-Cadherin Switch in Epithelial-to-Mesenchymal Transition: Signaling, Therapeutic Implications, and Challenges. Cells. 2019; 8: 1118.

26. Hollestelle A, Peeters JK, Smid M, Timmermans M, Verhoog LC, Westenend PJ, et al. Loss of E-cadherin is not a necessity for epithelial to mesenchymal transition in human breast cancer. Breast Cancer Res Treat. 2013;138:47-57.

27. Faria MH, Gonçalves BP, do Patrocínio RM, de Moraes-Filho MO, Rabenhorst SHB. Expression of Ki-67, topoisomerase II alpha and c-MYC in astrocytic tumors: correlation with the histopathological grade and proliferative status. Neuropathol. 2006;26:519–527.

28. Gurel B, Iwata T, Koh CM, Jenkins RB, Lan F, Dang CV, et al. Nuclear MYC protein overexpression is an early alteration in human prostate carcinogenesis. Mod Pathol. 2008; 21: 1156–1167.

29. Deng L, Xiong P, Luo Y, Bu X, Qian S, Zhong W, et al. Association between *IDH1/2* mutations and brain glioma grade. Oncol Lett 2018; 16: 5405-5409.

30. Huang J, Yu J, Tu L, Huang N, Li H, Luo Y. Isocitrate Dehydrogenase Mutations in Glioma: From Basic Discovery to Therapeutics Development. Front Oncol. 2019;9:506.

Acknowledgement:

Conflict of Interest: Authors declare No Conflict of Interest

Funding Source:

Legends

Table 1. Clinical and Pathological Characteristics of the Glioma Patients

Table 2. Frequency of IDH1/2 Mutations and 1p/19q Co-deletion Status in Malignant Glioma

Table 3. Association of Clinical and Molecular Pathology Features of Malignant Glioma with Proliferation rate of Primary Culture

Table 4. Inhibitory Concentration (IC50) of Temozolomide in the Primary Glioma Cells by MTT assay

Figure 1. Phenotype of Primary Glioma Cells. Phase-contrast microscopic images depicting the morphology of glioma cells belonging to different grades

Figure 2A. Grade-wise distribution of High and Low-Proliferating Cultures in absolute numbers. Cell cultures were assigned to the group with high-proliferation rate when the doubling time was less than 72h and to the group with low-proliferation rate when the doubling time was more than 72h.

Figure 2B. Population Doubling Time. Mean Population doubling time are displayed grade-wise as a Line Graph. The doubling time for each samples was determined three times and the values are represented as mean doubling time (h) ± standard deviation (SD). *$p < 0.05$; ** $p < 0.01$

Figure 3: Immunocytochemical Evaluation and representative Immuno-staining of GMT and Oncogenic Markers. Fluorescent microscope images show the cell nuclei labelled with DAPI (Blue) and GMT/Oncogenic Markers labelled with respective antibodies (Green, Alexaflour 488) and grouped grade-wise as per their proliferation rate. All images were captured at the Magnification of 10X x 10.

Figure 4: Simple Linear Regression analysis. Association between proliferation rate of the primary glioma culture and pathological characteristics such as IDH1/2 mutation, 1p/19q Co-deletion and expression levels of tumour markers such as MIB1 and p53.

Table 1

Clinical and Pathological Characteristics of the Glioma Patients

S. No	Age	Sex	Histology	Location	Grade	IDH1R132H	IDH1R132C	IDH1R100	IDH2R172	1p/19q Co-deletion	P53	MIB1
1.	55	M	Glioblastoma	Left temporal	IV	Negative	Negative	Negative	Negative	Negative	Negative	Positive (3+)
2.	35	M	Diffuse astrocytoma	Left frontotemporal	II	Positive	Negative	Negative	Negative	Negative	Positive	Negative
3.	30	F	Anaplastic astrocytoma	Right temporal	III	Negative	Negative	Negative	Negative	Negative	Positive	Positive (2+)
4.	29	M	Oligodendroglioma	Right frontal	II	Positive	Negative	Negative	Negative	Positive	Negative	Negative
5.	39	M	Diffuse astrocytoma	Right temporal	II	Positive	Negative	Negative	Negative	Positive	Positive	Negative
6.	55	M	Glioblastoma	Right parietal	IV	Negative	Negative	Negative	Negative	Negative	Negative	Negative
7.	66	F	Glioblastoma	Right parieto occipital	IV	Negative	Negative	Negative	Negative	Negative	Positive	Positive (2+)
8.	59	M	Glioblastoma	Left fronto temporal	IV	Negative	Negative	Negative	Negative	Negative	Positive	Positive (3+)
9.	45	M	Diffuse astrocytoma	Left frontal	II	Positive	Negative	Negative	Negative	Negative	Negative	Negative
10.	48	F	Glioblastoma	Left temporal	IV	Negative	Negative	Negative	Negative	Negative	Negative	Positive (1+)
11.	19	F	Anaplastic astrocytoma	Right parietal	III	Negative	Negative	Negative	Negative	Negative	Positive	Positive (2+)
12.	59	M	Glioblastoma	Corpus callosal	IV	Negative	Negative	Negative	Negative	Negative	Negative	Positive (1+)
13.	63	M	Glioblastoma	Right temporal	IV	Negative	Negative	Negative	Negative	Negative	Negative	Positive (2+)
14.	50	M	Anaplastic astrocytoma	Right parietal	III	Negative	Negative	Negative	Negative	Negative	Positive	Positive (3+)
15.	71	F	Glioblastoma	Right temporal	IV	Negative	Negative	Negative	Negative	Negative	Negative	Positive (2+)
16.	47	F	Glioblastoma	Left parietal	IV	Negative	Negative	Negative	Negative	Negative	Negative	Positive (2+)
17.	37	M	Diffuse astrocytoma	Right parieto occipital	II	Positive	Negative	Negative	Negative	Negative	Positive	Negative
18.	44	M	Diffuse astrocytoma	Right temporoparietal	II	Positive	Negative	Negative	Negative	Positive	Positive	Negative
19.	38	M	Oligo astrocytoma	Right frontoparietal	II	Positive	Negative	Negative	Negative	Positive	Negative	Negative
20.	69	M	Glioblastoma	Right temporal	IV	Negative	Negative	Negative	Negative	Negative	Positive	Positive (1+)
21.	54	M	Anaplastic astrocytoma	Right frontal	III	Negative	Negative	Positive	Negative	Positive	Positive	Positive (1+)
22.	38	M	Diffuse astrocytoma	Right temporoccipital	II	Positive	Negative	Negative	Negative	Negative	Negative	Negative
23.	71	M	Anaplastic astrocytoma	Left temporoparietal	III	Negative	Negative	Negative	Negative	Negative	Positive	Positive (1+)
24.	30	M	Anaplastic astrocytoma	Right caudate	III	Negative	Negative	Negative	Negative	Negative	Positive	Positive (2+)
25.	53	M	Glioblastoma	Left frontal	IV	Negative	Negative	Negative	Negative	Negative	Negative	Positive (2+)
26.	45	M	Anaplastic astrocytoma	Right frontal	III	Negative	Negative	Negative	Negative	Negative	Positive	Positive (2+)
27.	63	M	Glioblastoma	Left temporal	IV	Negative	Negative	Negative	Negative	Negative	Positive	Positive (3+)

28.	64	M	Glioblastoma	Corpus callosum	IV	Negative	Negative	Negative	Negative	Negative	Negative	Positive (2+)
29.	47	M	Oligodendroglioma	Left parietal	II	Positive	Negative	Negative	Negative	Positive	Negative	Negative
30.	27	F	Diffuse astrocytoma	Right frontal	II	Negative	Positive	Negative	Negative	Negative	Negative	Negative
31.	57	M	Glioblastoma	Left insular	IV	Negative	Negative	Negative	Negative	Negative	Positive	Positive (1+)
32.	79	M	Glioblastoma	Right temporal	IV	Negative	Negative	Negative	Negative	Negative	Negative	Positive (1+)
33.	30	F	Diffuse astrocytoma	Left frontal	II	Negative	Positive	Negative	Negative	Negative	Positive	Negative
34.	58	F	Glioblastoma	Right temporal	IV	Negative	Negative	Negative	Negative	Negative	Negative	Positive (2+)
35.	37	F	Oligodendroglioma	Right frontal	II	Positive	Negative	Negative	Negative	Positive	Negative	Negative
36.	67	F	Glioblastoma	Left motor cortex	IV	Negative	Negative	Negative	Negative	Negative	Positive	Positive (1+)
37.	66	F	Glioblastoma	Right parieto occipital	IV	Negative	Negative	Negative	Negative	Negative	Positive	Positive (2+)
38.	74	M	Glioblastoma	Left fronto parietal	IV	Negative	Negative	Negative	Negative	Negative	Negative	Positive (1+)
39.	27	M	Glioblastoma	Right temporal	IV	Negative	Negative	Negative	Negative	Negative	Positive	Positive (1+)
40.	56	M	Glioblastoma	Left frontal	IV	Negative	Negative	Negative	Negative	Negative	Positive	Positive (2+)
41.	53	F	Oligodendroglioma	Right Parietal	II	Positive	Negative	Negative	Negative	Positive	Negative	Negative
42.	43	M	Anaplastic astrocytoma	Left frontal	III	Negative	Negative	Negative	Negative	Negative	Negative	Positive (2+)
43.	37	M	Oligodendroglioma	Right temporoparietal	II	Positive	Negative	Negative	Negative	Negative	Positive	Negative
44.	54	M	Glioblastoma	Right frontal	IV	Negative	Negative	Negative	Negative	Negative	Negative	Positive (3+)
45.	61	M	Anaplastic astrocytoma	Right temporal	III	Negative	Negative	Negative	Negative	Negative	Positive	Positive (2+)

Relevant clinical data concerning age (at the time of admission), gender (M = male; F = female), tumor histology, grade and localization, IDH1/2 mutation and 1p/19q co-deletion status along with presence/absence of proliferation marker MIB1 and Tumor Suppressor Marker p53 are summarized.

Table 2

Frequency of IDH1/2 Mutations and 1p/19q Co-deletion Status in Malignant Glioma

Mutations	Grade II		Grade III		Grade IV	
	HP Cultures	LP Cultures	HP Cultures	LP Cultures	HP Cultures	LP Cultures
Total Patients	7	5	4	3	8	13
IDH1R132H	6	4	0	0	0	0
IDH1R132C	1	1	0	0	0	0
IDH1R100	0	0	1	0	0	0
1p/19q codeletion	2	4	1	0	0	0

HP Cultures – High Proliferating Cultures; LP Cultures – Low Proliferating Cultures

Table 3

Association of Clinical and Molecular Pathology Features of Malignant Glioma with Proliferation rate of Primary Culture

	High Proliferation Culture	Low Proliferation Culture	$\chi 2$	*p value*
Total number of cases	19 (47%)	21 (53%)	–	–
Gender (Female/Male)	4/15	8/13	1.3796	0.2402
Age at diagnosis (years)	52.53 ± 15.45	47.77 ± 15.17	–	0.3316[$]
IDH1R132 (Positive/Negative)	7/12	3/18	2.7068	0.0999
IDH1R132H (Positive/Negative)	6/13	4/17	1.6708	0.1961
IDH1R132C (Positive/Negative)	1/18	1/20	0.0053	0.9421
IDH1R100 (Positive/Negative)	1/18	0/21	0.4699	0.4930
1p/19q co-deletion (Positive/Negative)	2/17	6/15	3.9665	0.0497*
p53 (Positive/Negative)	14/5	6/15	8.1203	0.0044*
MIB1 (Positive/Negative)	12/7	15/6	0.3110	0.5770

[$] Students ‘t’ test; * statistically significant at $p < 0.05$

Table 4

Inhibitory Concentration (IC50) of Temozolomide in the Primary Glioma Cells by MTT assay

Primary Glioma Cells	IC50 of Temozolomide (mM)		*p* value
	High Proliferating Cultures	Low Proliferating Cultures	
Grade II	3.110 ± 0.311	1.212 ± 0.209	0.00473
Grade III	13.29 ± 0.817	4.519 ± 0.532	0.00001
Grade IV	9.663 ± 1.134	1.447 ± 0.471	0.00001

Cell viability was measured after a 48h treatment with the indicated concentration of Temozolomide (as mentioned in the materials and methods. Results are the mean ± Standard Deviation (SD).

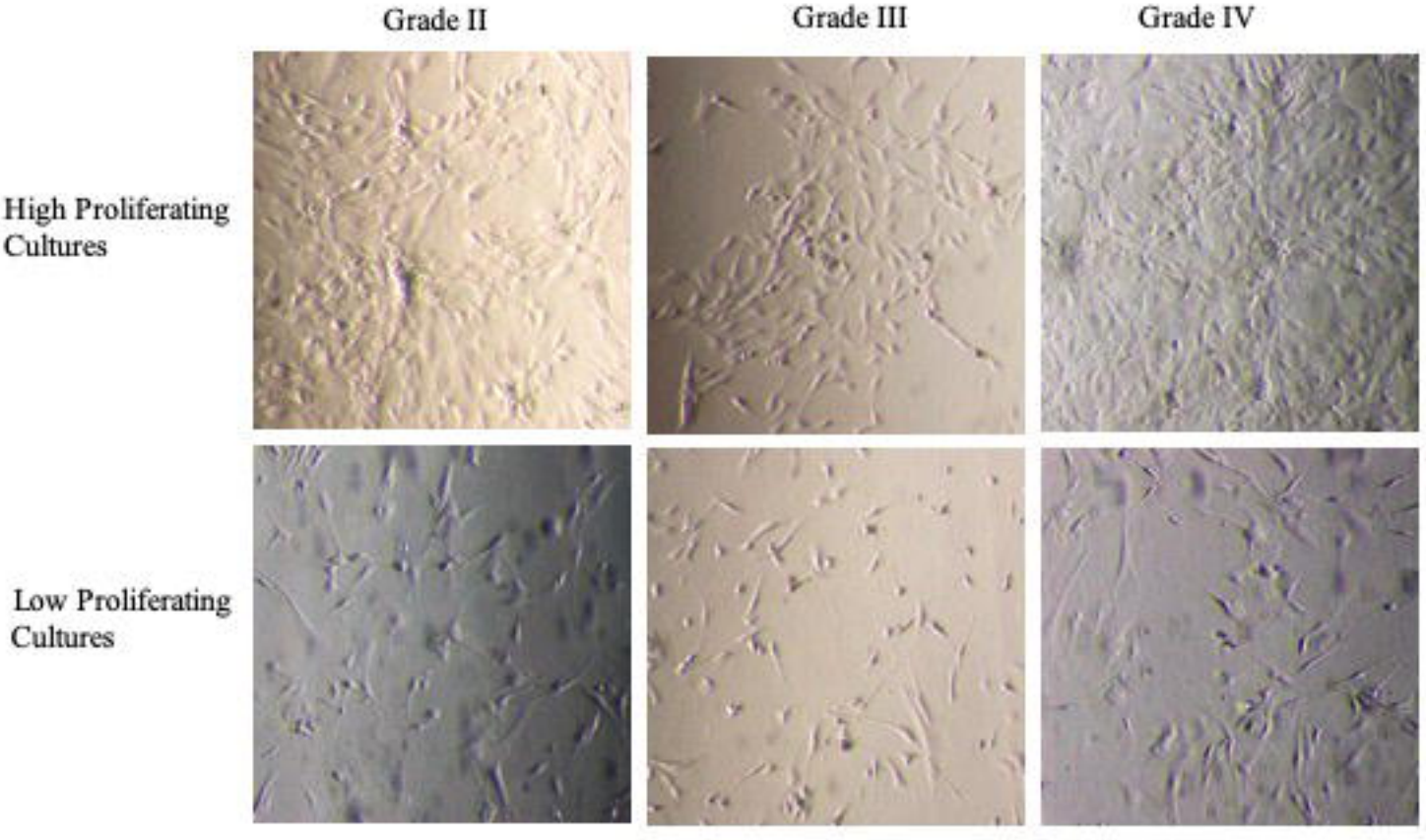
Grade II
Grade III
Grade IV
High Proliferating Cultures
Low Proliferating Cultures

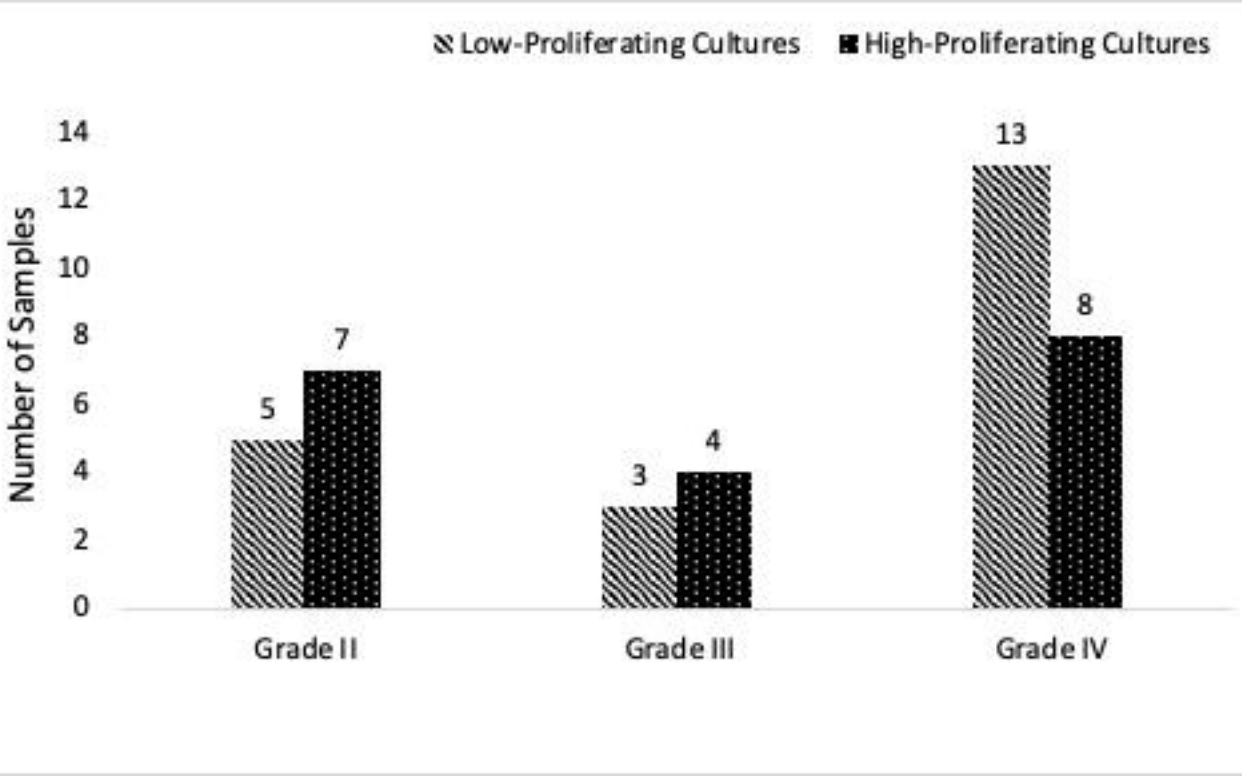
Low-Proliferating Cultures
High-Proliferating Cultures
Number of Samples
14
12
10
8
6
4
2
0
5
7
3
4
13
8
Grade II
Grade III
Grade IV

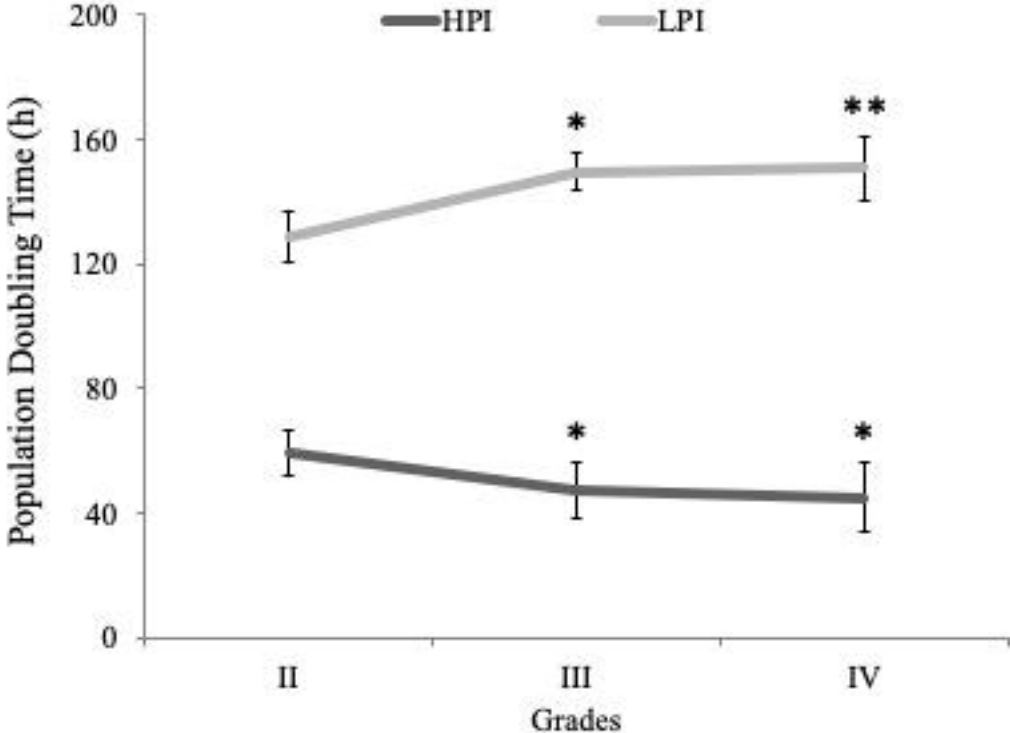
HPI
LPI
Population Doubling Time (h)
200
160
120
80
40
0
*
**
*
*
II
III
IV
Grades

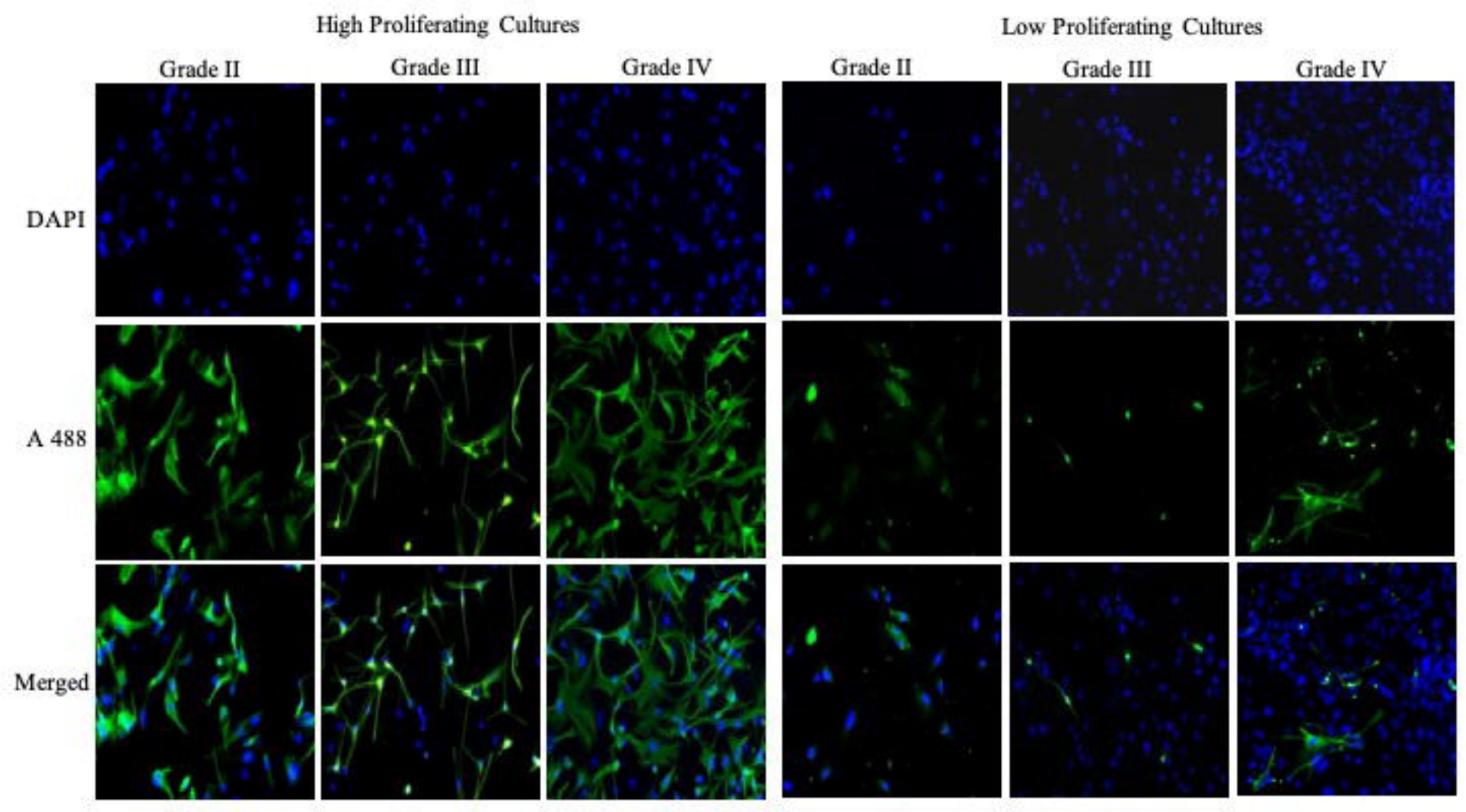
High Proliferating Cultures
Low Proliferating Cultures
Grade II
Grade III
Grade IV
Grade II
Grade III
Grade IV
DAPI
A 488
Merged

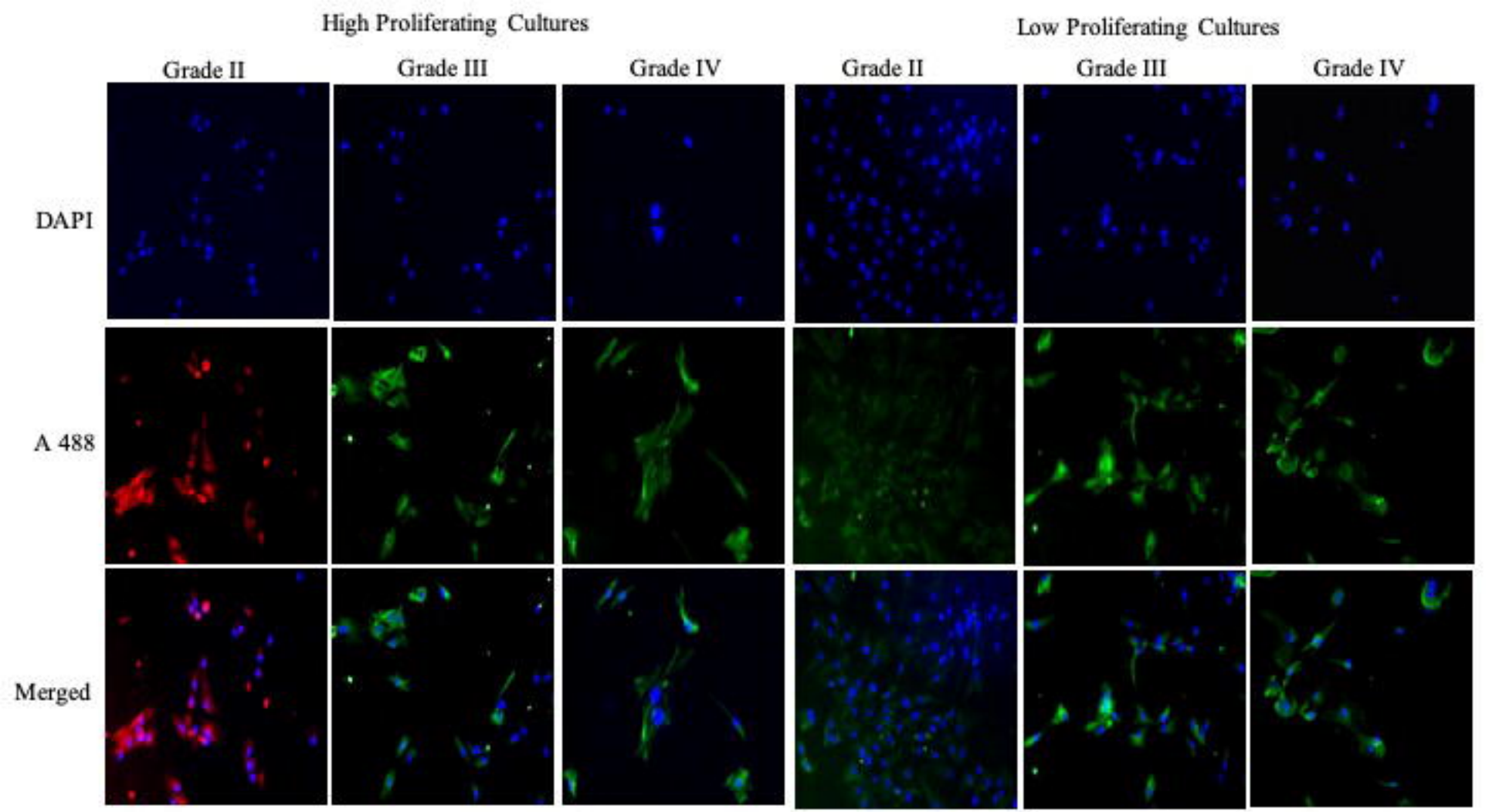
High Proliferating Cultures
Low Proliferating Cultures
Grade II
Grade III
Grade IV
Grade II
Grade III
Grade IV
DAPI
A 488
Merged

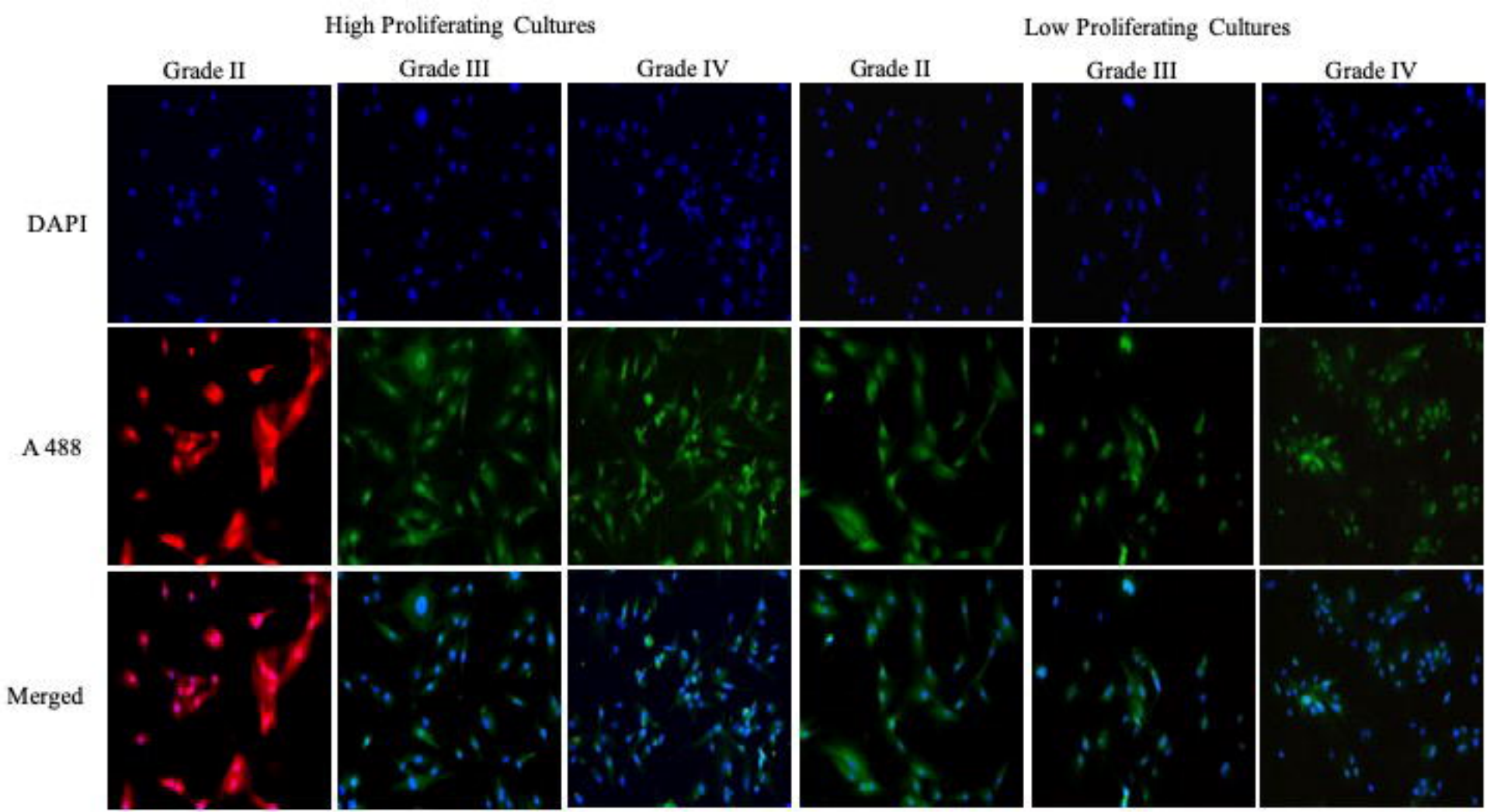
High Proliferating Cultures
Low Proliferating Cultures
Grade II
Grade III
Grade IV
Grade II
Grade III
Grade IV
DAPI
A 488
Merged

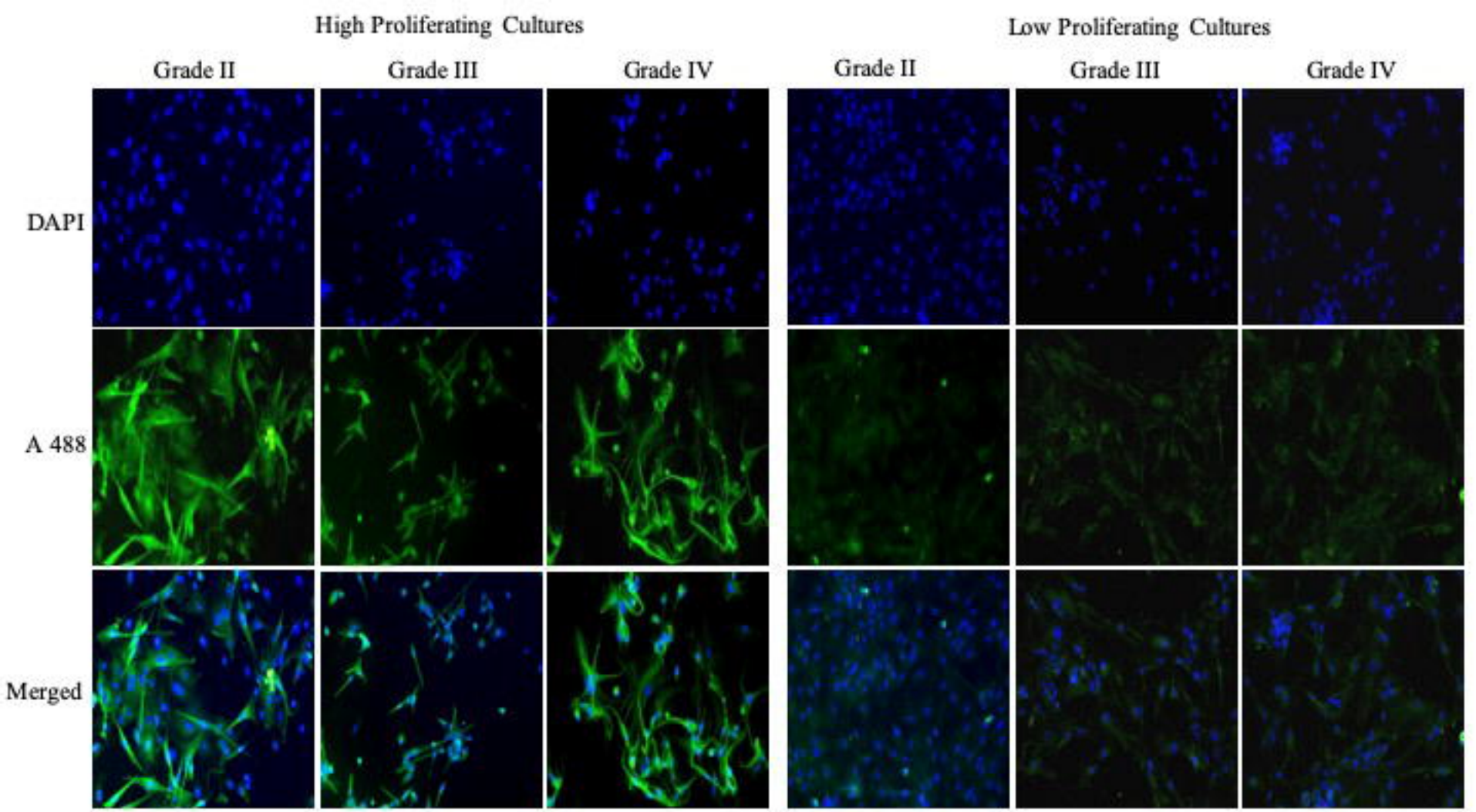
High Proliferating Cultures
Low Proliferating Cultures
Grade II
Grade III
Grade IV
Grade II
Grade III
Grade IV
DAPI
A 488
Merged

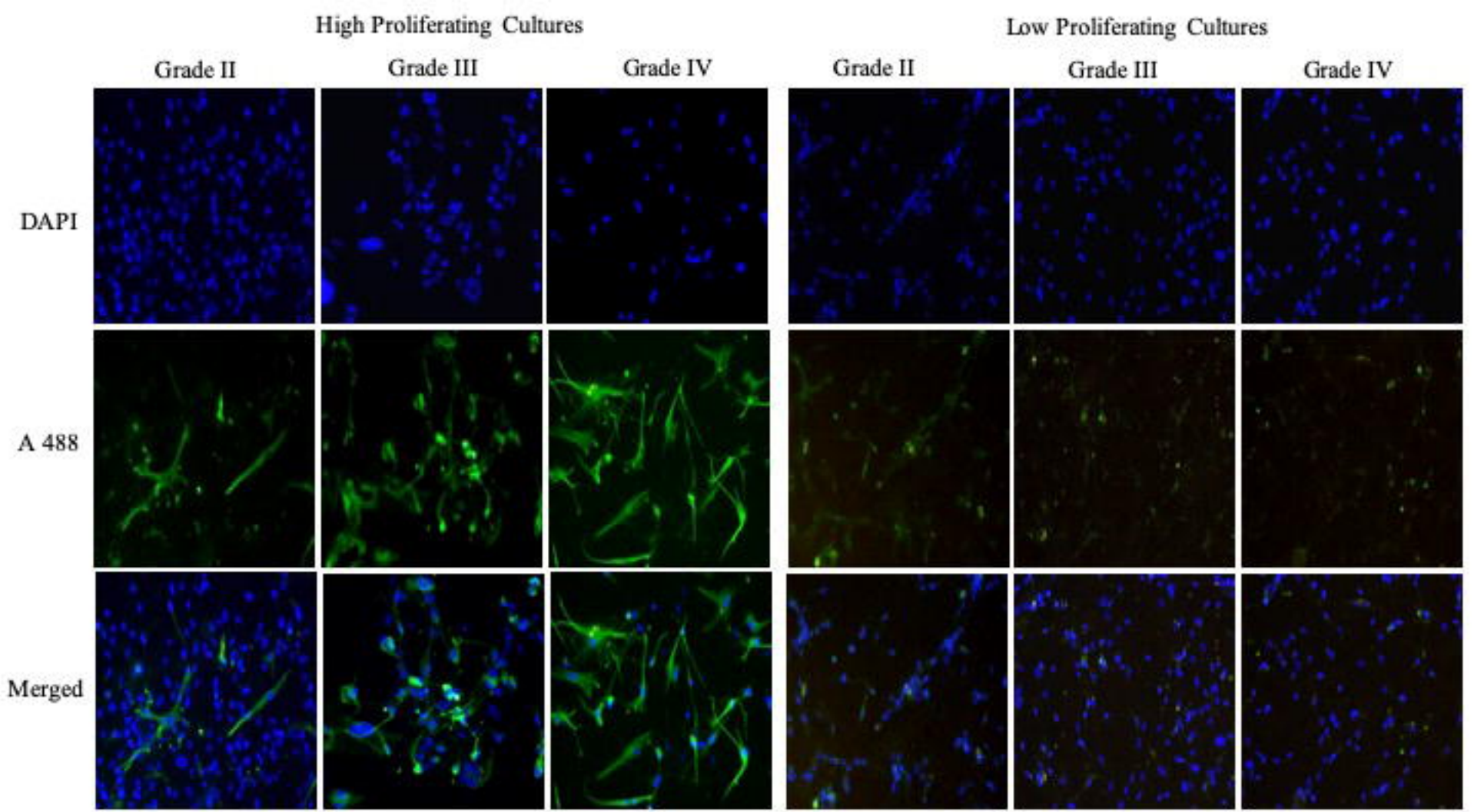
High Proliferating Cultures
Low Proliferating Cultures
Grade II
Grade III
Grade IV
Grade II
Grade III
Grade IV
DAPI
A 488
Merged

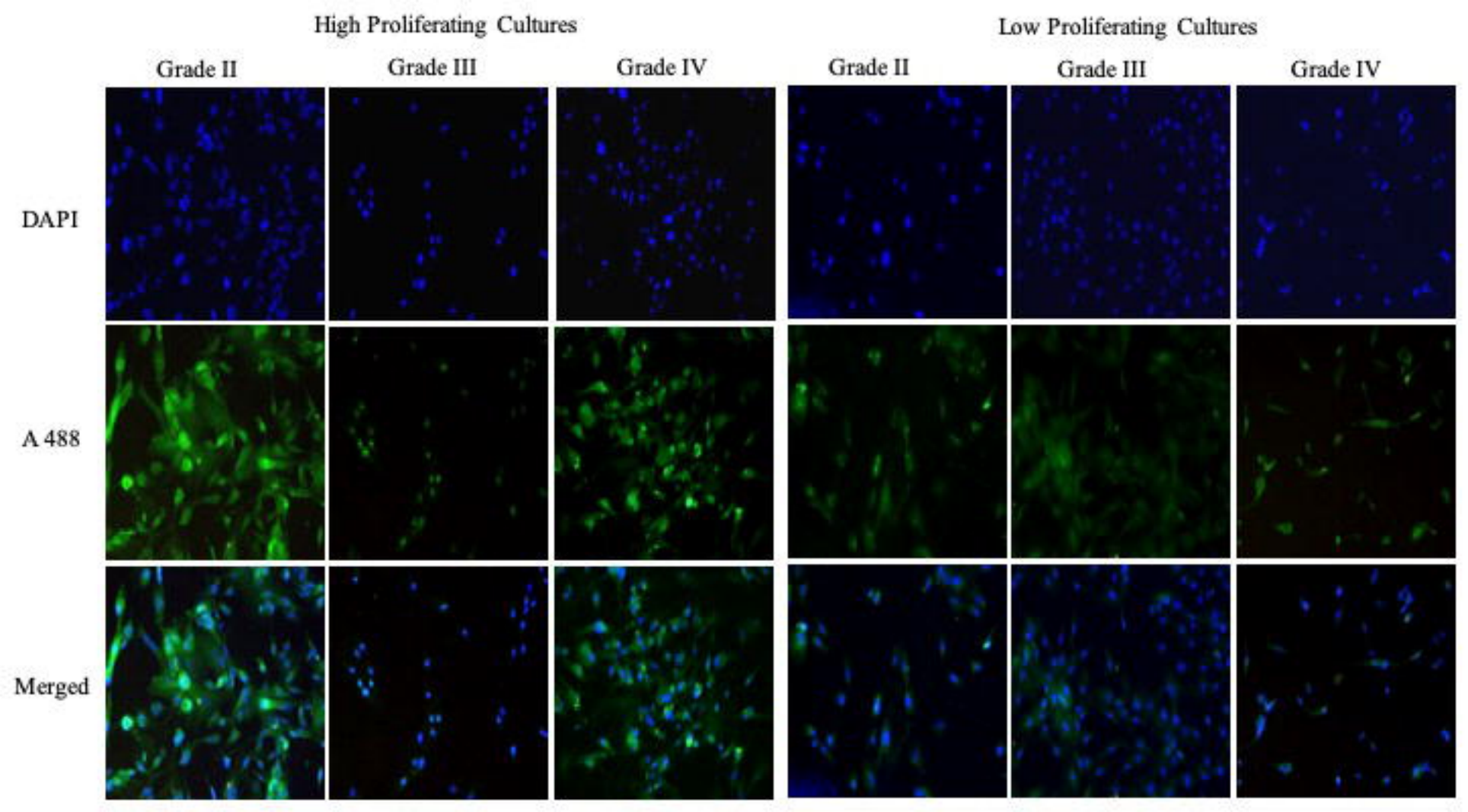
High Proliferating Cultures
Low Proliferating Cultures
Grade II
Grade III
Grade IV
Grade II
Grade III
Grade IV
DAPI
A 488
Merged

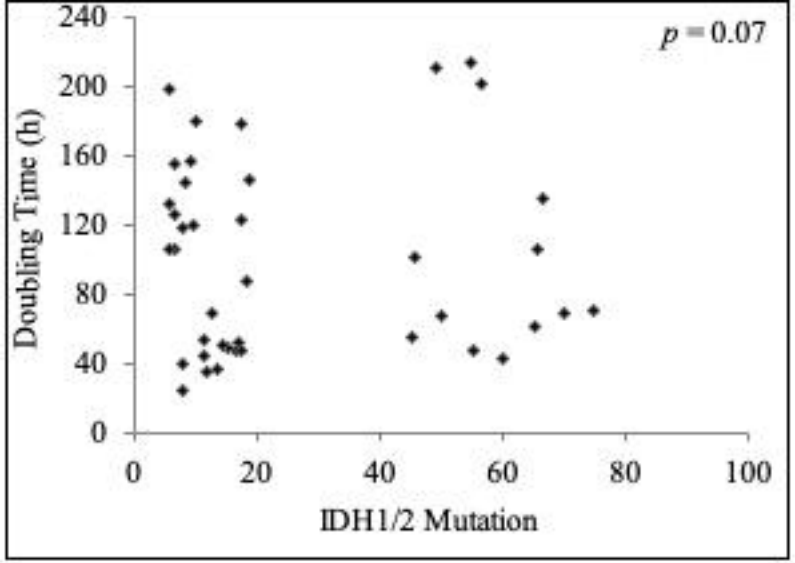
p = 0.07
Doubling Time (h)
240
200
160
120
80
40
0
0
20
40
60
80
100
IDH1/2 Mutation

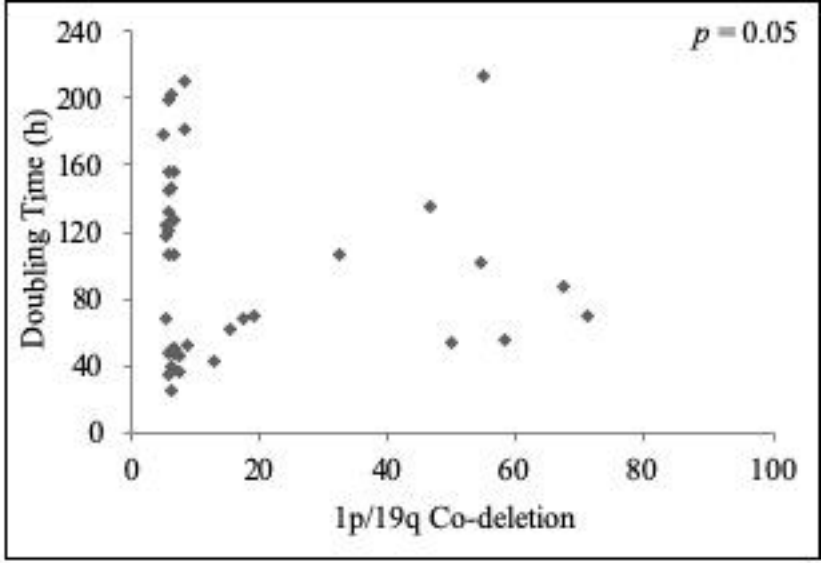
p = 0.05
Doubling Time (h)
240
200
160
120
80
40
0
0
20
40
60
80
100
1p/19q Co-deletion

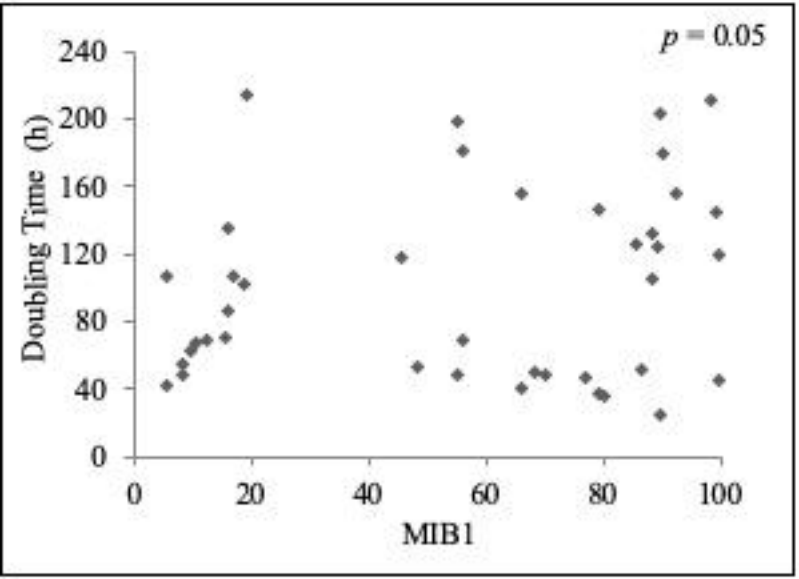
p = 0.05
Doubling Time (h)
240
200
160
120
80
40
0
0
20
40
60
80
100
MIB1

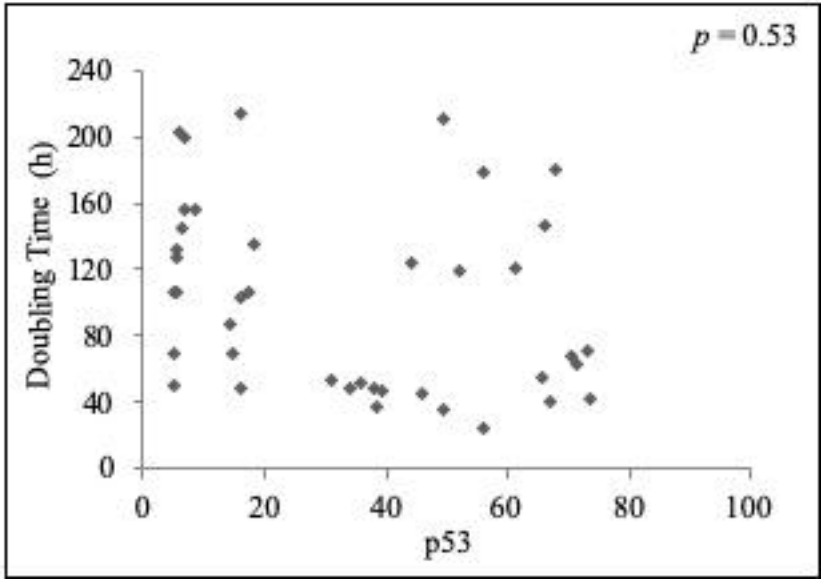
p = 0.53
Doubling Time (h)
240
200
160
120
80
40
0
0
20
40
60
80
100
p53